OPTICAL AND STRUCTURAL PERFORMANCE OF NANOSTRUCTURED Te THIN FILMS BY (CSP) WITH VARIOUS THICKNESSES

S. S. CHIAD [a], H. A. NOOR[b], O. M. ABDULMUNEM[c], N. F. HABUBI [a], M. JADAN[d], J. S. ADDASI[e,*]

[a]*Department of Physics, College of Education, Mustansiriyah University, Iraq*
[b]*Department of Physics, College of Education, University of Al- Qadisiyah, Al-Qadisiya, Iraq*
[c]*Department of Physics, College of Science, Mustansiriyah University, Iraq*
[d]*Department of Physics, College of Science, Imam Abdulrahman Bin Faisal University, P.O. Box 1982, 31441 Dammam, Saudi Arabia*
[e]*Department of Applied Physics, College of Science, Tafila Technical University, 66110 Tafila, Jordan*

In this study, were investigated structural, optical properties and morphological of Te Nano-thin films with different thicknesses by Chemical spray pyrolysis (CSP) method. The structural properties of the films were studied as a Te dopant at 150-450 thicknesses. The films were characterized by XRD to study film structure. It was observed that the hexagonal wurtzite structure of ZnO for all samples. The films exhibited wurtzite (102) preferential growth in different thicknesses. Grain size values calculated from Scherrer's formula, were varied in range of (96-84) nm. The band gap energy values were calculated respectively for Te thickness samples.

(Received October 8, 2019; Accepted January 17, 2020)

Keywords: Thin film thickness, Te by CSP, XRD Nano films, Te properties

1. Introduction

Tellurium semiconductor is vastly used in devices like Gas sensors and Air products. Energy band of Te is 0.368 eV [1, 2]. Many techniques have devoted to prepare Te thin films like molecular beam epitaxy, solution growth [3-7]. Chemical spray deposition is a low cost and convenient method has recently been utilized to prepare thin polycrystalline films of a wide variety of compound semiconductors by a number of investigators among them [8, 9].

Thickness is one of these parameters that have a significant effect on the structural, optical and electrical properties of materials. According to material's thickness, it can be classified into thin film, thick film and bulk. Each one may characterizes by certain structural properties; amorphous, polycrystalline and/or crystalline state [10].

The aim of this work is to prepare Te thin films with different thicknesses via CSP and study their structural, topographical and optical properties.

2. Experimental procedure

Tellurium films were deposited onto a preheated glass substrate CSP. 0.1 M of Tellurium tetrachloride dissolved in redistilled water was considering as a starting solution to form Te thin films. Different thicknesses (150, 300, 450) nm of Te was obtained. The optimal preparation conditions were fixed after many tests and they found to be: substrate temperature was kept at 400 ^{O}C through deposition process. Carrier gas was Nitrogen. Deposition rate was 6 mL/min, spryer rate was 10 s lasted by 45 Sec to prevent high cooling. Space among substrate and nozzle was kept

* Corresponding author: addasijihad@gmail.com

at 28 cm. The XRD (SHIMADZU XRD-6000) was used to determine the nature of the film structure, Film morphology was determined by AFM (AA3000 SPM).

Table 1. The preparation conditions for the as deposited thin films.

Substrate temperature	400 °C
Substrate to sprayer nozzle distance	29 cm
Sprayer rate	5 mL/min
Sprayer time	8 S
Stopping interval time	1 min

3. Results and discussion

3.1. The structure characterization

The crystal structure and orientation of Te Nano thin-films thickness were inspected by XRD patterns. Figure 1 shows Te patterns for 150, 300 and 450 nm thicknesses. These spectra indicated that the films had polycrystalline nature.

Te hexagonal array structure (JCPDS card file no. 36-1451) with a peak of (102), the peak of (102) were almost splits with Te thickness. The most peak intensity was (102) for all samples. The highest peak intensity of (102) was also observed when Te thickness ratios were 300 nm and 450 nm. For a peak of (102), the average crystallite sizes (D) was calculated by using the following Scherrer's formula [11]:

$$D = \frac{0.9\lambda}{\beta cos\theta} \qquad (1)$$

where, λ is X-rays wavelength, β was (FWHM) in radians and θ was angle of diffraction. Grain size value of Te decreased from 96 nm to 84 nm with increasing Te-Thickness. Dislocation density (δ) is amount of defect measuring, which was estimated using equation 2 [12, 13].

$$\delta = \frac{1}{D^2} \qquad (2)$$

Dislocation density values (δ) showed increasing tendency with increasing Te thickness.

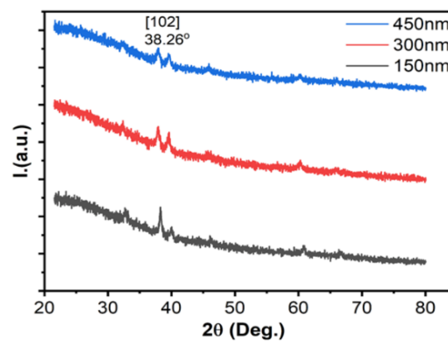

Fig. 1. XRD patterns of deposited films.

Table 2. Structural data of deposited films.

Te (nm) Thickness	(hkl) Plane	2Θ (Deg.)	Lattice constants		FWHM (Deg.)	D (nm)	ε x10^{-4}	(δ) 10^{-4} $(1/nm)^2$
			a (Å)	c (Å)				
150	(102)	38.26	4.457	5.927	0.26319	31.95	11.46	9.79
300	(102)	38.26	2.665	4.947	0.45311	18.55	19.74	29.033
450	(102)	38.26	3.249	5.206	0.50905	16.52	22.17	36.64

3.2. Optical properties

Optical transmission (T) spectra of doped and undoped samples were shown in Fig. 2. From transmittance spectra, there was reduction continuously with Te doping at all wavelength ranges. The optical transmission shifted red within increasing tellurium content. The transmittance in the short wavelengths showed decreasing tendency with increasing Te concentration. The decreasing transmittance with Te dopants were observed by [14]. The absorption coefficient (α) of films was specified by equation [15]:

$$\alpha = \frac{\ln(1/T)}{d} \tag{3}$$

where d is film thickness. Fig. 3 represents α that assure direct transition.

The optical band gap was evaluated from next relation [16, 17]:

$$\alpha h\nu = A(h\nu - E_g)^{\frac{1}{2}} \tag{4}$$

where $h\nu$ was photon energy and A the constant, respectively. The values of E_g for Te were determined by plotting in Fig. 4 were found as (250-700) nm. From the results illustrate, when Te thickness is increased the band gap of Te continuously decreased [18].

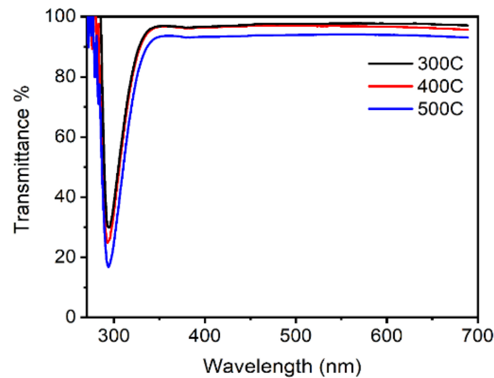

Fig. 2. Transmittance versus wavelength of deposited films.

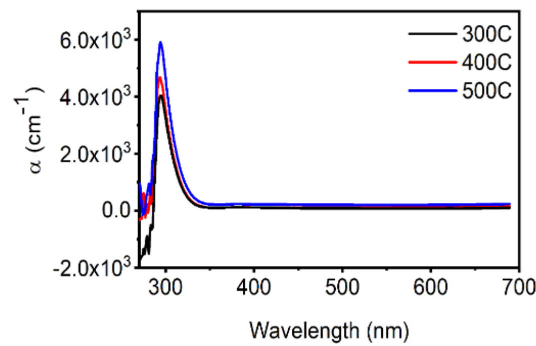

Fig. 3. α versus wavelength of deposited films.

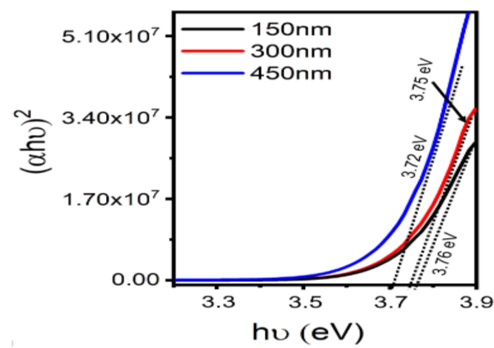

Fig. 4. E_g of deposited films.

3.3. AFM Results

Surface morphology roughness was studied by AFM technique. Fig. 5 show AFM images Te films with thickness 150 nm and 450 nm. It discloses that Te films have a fine surface topography, which decreases with Te thickness increasing. The decrease of surface roughness may be assigned to the big grain formation. Fig. 5 shows the root-mean-square (RMS) of average surface roughness, particle or grain size, and 3D surface morphology. Moreover, in Table 3 determined rough parameters data, it's evident that (RMS) decreased significantly with increment of thickness.

Table 3. Surface morphology of deposited films.

Te: Thickness (nm)	Avg. Diameter (nm)	Average roughness (nm)	R. M. S. (nm)
150	96.93	9.67	11.2
300	88.95	7.93	9.49
450	84.78	3.99	4.69

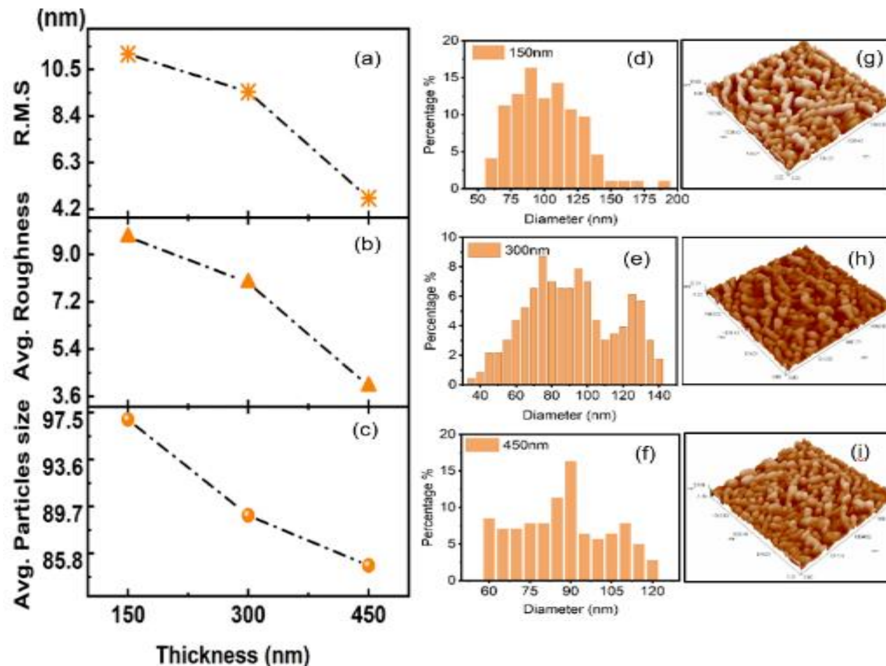

Fig. 5. AFM, RMS, Roughness Average and Avg. Diameter for different thickness, Histography and AFM images of the Te topography for different thickness (d, g) 150 nm (e, h) 300 nm and (f, i) 450 nm.

4. Conclusions

Te Nano-thin films were prepared on glass substrates by the (CSP) technique. Effects of thickness condition on structural, optical properties and surface morphology of films were studied. XRD were showed the polycrystalline with orientation (102) of Te: Nano-thin films. Surface morphologies of this showed average roughness 9.67 nm and diameter of about 96.93 nm.

Acknowledgments

Authors would like to extend their thanks and gratitude to the Department of Physics at the College of Science of the Mustansiriyah University.

References

[1] R. Venkatasubramanian, E. Siivola, T. Colpitts and B. O'Quinn, Nature **413**, 597 (2001).
[2] D. H. Rose, F. S. Hasoon, R. G. Dhere, D. S. Albin, R. M. Ribelin, X. S. Li, Y. Mahathongdy T. M. Gessert, P. Sheldon, Prog Photovoltaics Res. Appl. **7**, 331 (1991).
[3] V. Barrioz, G. Kartopu, S. J. C. Irvine, S. Monir, X. Yang, J. Cryst. Growth **354**, 81 (2012).
[4] Y. Al-Douri, M. Ameri, A. Bouhemadou, Microsyst. Technol. **22**, 2529 (2016).
[5] Swati Arora, Vivek Jaimini, Subodh Srivastava, Y. K. Vijay, Journal of Nanotechnology Article ID 4276506 (2017).
[6] S. K. Lu, J. T. Huang, T. H. Lee, J. J. Wang, D. S. Liu, Smart Sci. **2**, 7 (2014).
[7] A. Iribarren, P. Fermandez, J. Piqueras, J. Mater. Sci. **43**, 2844 (2008).
[8] B. M. Celalettin, O. Nilgun, Thin Solid Films **518**, 1925 (2010).
[9] H. S. Janan, A. H. Abdulkhadhim, International Journal of Applied Mathematics, Electronics and Computers **3**(2), 96 (2015).
[10] A. El-Denglawey, M. M. Makhlouf, M. Dongol, Results in Physics **10**,714 (2018).

[11] S. S. Chiad, Kh. H. Abass, T. H. Mubarak, N. F. Habubi, M. K. Mohammed, A. A. Khadayeir, Journal of Global Pharma Technology **11**(4), 369 (2019).
[12] K. Ravichandran, G. Muruganantham, B. Sakthivel, Physica B: Condensed Matte **404**(21), 4299 (2009).
[13] E. S. Hassan, T. H. Mubarak, Kh. H. Abass, S. S. Chiad, N. F. Habubi, M. H. Rahid, A. A. Khadayeir, M. O. Dawod, I. A. Al-Baidhany, Journal of Physics: Conference Series **1234** (2019).
[14] H. L. Pan, B. Yao, M. Ding, R. Deng, T. Yang, Y. R. Sui, L. L. Gao, J. Non-Cryst. Sol. **356**, 906 (2010).
[15] A. A. Khadayeir, E. S. Hassan, S. S. Chiad, N. F. Habubi, Kh. H. Abass, M. H. Rahid, T. H. Mubarak, M. O. Dawod, I. A. Al-Baidhany, Journal of Physics: Conference Series **1234** (2019).
[16] J. Tauc, R. Grigorovici, A. Vancu, Phys. Status Solidi B **15**, 627 (1966).
[17] A. Sh. Alkelaby, Kh. H. Abass, T. H. Mubarak, N. F. Habubi, S. S. Chiad, I. Al-Baidhany, Journal of Global Pharma Technology **11**(4), 347 (2019).
[18] A. Swati, Y. K. Vijay, AIP Conference Proceedings **1953**(1) AIP Publishing (2018).